

LETTER TO THE EDITOR

SOFIA observations of far-infrared hydroxyl emission toward classical ultracompact HII/OH maser regions

T. Csengeri¹, K. M. Menten¹, F. Wyrowski¹, M. A. Requena-Torres¹, R. Güsten¹, H. Wiesemeyer¹, H.-W. Hübers^{2,3}, P. Hartogh⁴, and K. Jacobs⁵

¹ Max-Planck-Institut für Radioastronomie, Auf dem Hügel 69, D-53121 Bonn, Germany e-mail: [ctimea;kmenten]@mpi.fr.de

² Deutsches Zentrum für Luft- und Raumfahrt, Institut für Planetenforschung, Rutherfordstraße 2, 12489 Berlin, Germany

³ Institut für Optik und Atomare Physik, Technische Universität Berlin, Hardenbergstraße 36, 10623 Berlin, Germany

⁴ Max-Planck-Institut für Sonnensystemforschung, Max-Planck-Straße 2, 37191 Katlenburg-Lindau, Germany

⁵ I. Physikalisches Institut, Universität zu Köln, Zùlpicher Str. 77, 50937 Köln, Germany

Received ... ; accepted

ABSTRACT

Context. The hydroxyl radical (OH) is found in various environments within the interstellar medium (ISM) of the Milky Way and external galaxies, mostly either in diffuse interstellar clouds or in the warm, dense environments of newly formed low-mass and high-mass stars, i.e. in the dense shells of compact and ultracompact HII regions (UCHIRs). Until today, most studies of interstellar OH involved the molecule's radio wavelength hyperfine structure (hfs) transitions. These lines are generally not in local thermodynamical equilibrium (LTE) and either masing or over-cooling complicates their interpretation. In the past, observations of transitions between different rotational levels of OH, which are at far-infrared wavelengths, have suffered from limited spectral and angular resolution. Since these lines have critical densities many orders of magnitude higher than the radio wavelength ground state hfs lines and are emitted from levels with more than 100 K above the ground state, when observed in *emission*, they probe very dense and warm material.

Aims. We aim to probe the warm and dense molecular material surrounding the UCHIR/OH maser sources W3(OH), G10.62–0.39 and NGC 7538 IRS1 by studying the ${}^2\Pi_{1/2}, J = 3/2 - 1/2$ rotational transition of OH in emission and, toward the last source also the molecule's ${}^2\Pi_{3/2}, J = 5/2 - 3/2$ ground-state transition in absorption.

Methods. We used the Stratospheric Observatory for Infrared Astronomy (SOFIA) to observe these OH lines, which are near 1.84 THz (163 μm) and 2.51 THz (119.3 μm), with high angular ($\sim 16''/11''$) and spectral resolution (better than 1 km s^{-1}).

Results. We clearly detect the OH lines, some of which are blended with each other. Employing non-LTE radiative transfer calculations we predict line intensities using models of a low OH abundance envelope versus a compact, high-abundance source corresponding to the origin of the radio OH lines. From the observed velocities and line-widths we can place constraints on the origin of the emission, and with detailed modeling we show for instance that the OH emission of W3(OH) comes from the UCHIR and not from the envelope of the nearby hot-core.

Conclusions. The far-IR lines of the OH molecule provide important information on the density and temperature structure of UCHIRs. Taking a low-abundance envelope component is not sufficient to reproduce the spectra for W3(OH) and G10.62–0.39, a compact, high OH column density source – corresponding to the OH radio emitting sources is definitively required.

Key words. Stars: formation – ISM: HII regions – ISM: molecules – Masers – Submillimeter: ISM

1. Introduction

The hydroxyl radical (OH) was the first interstellar molecule detected at radio wavelengths. After various searches, Weinreb et al. (1963) found absorption in the two strongest ($F = 2 - 2$ and $2 - 1$, near 1667 and 1665 MHz, respectively) of the hyperfine structure (hfs) transitions within the molecule's ${}^2\Pi_{3/2}, J = 3/2$ ground state toward the supernova remnant Cas A. Subsequent studies found absorption toward all four of the “18 cm lines” first toward the Galactic center (Gardner et al. 1964) and, later, many galactic lines of sight (e.g., Goss 1968). Soon, also *emission* near 1665 MHz was discovered toward prominent HII regions, i.e., sites of recent star formation (Weaver et al. 1965). This and the detection of weaker emission at the frequencies of the $F = 2 - 2$ and $1 - 2$ OH hfs lines (at 1667 and 1720 MHz) allowed Weinreb et al. (1965) to identify of OH as the carrier of this peculiar emission. It was readily identified as due to maser action by the latter authors because

of the observed peculiar profiles with multiple, narrow velocity components of polarized emission with highly anomalous relative hfs component intensity ratios, with the 1665 MHz $F = 2 - 1$ line usually being the strongest (Weinreb et al. 1965, Barrett & Rogers 1966). The maser nature was clinched by interferometry, which showed that the OH emission near the prominent HII region W3 had brightness temperatures exceeding 10^9 K and arose from compact ($< 0''.05$) spots spread over a few arc sec (thousands of AU) and significantly offset (by $14'$ or ≈ 8 pc) from the radio continuum emission maximum of the HII region (Rogers et al. 1966, Moran et al. 1967, Davies et al. 1967). Most interestingly, the maser position turned out to be consistent with that of a newly detected radio source much smaller than W3: the archetypical example of what Mezger et al. (1967), based on their 2 cm radio continuum observations, termed “a new class of compact H II regions associated with OH emission sources”. This source, W3(OH), is characterized by its youth (2300 yr, Kawamura & Masson

1998), compactness (~ 0.02 pc) and high electron densities ($\sim 2 \cdot 10^5 \text{ cm}^{-3}$, Dreher & Welch 1981) and is still surrounded by an expanding dusty, molecular envelope (e.g., Wyrowski et al. 1999). It is the archetypical ultracompact HII region (UCHIIR) and is discussed in this *Letter* along with the UCHIIRs G10.62–0.39 and NGC 7538 IRS1.

In addition to the lines from the ground state, transitions between hfs levels of various rotationally excited states with rotational quantum number J from $5/2$ to $9/2$ from the lower energy $^2\Pi_{3/2}$ ladder and from $1/2$ to $5/2$ in the $^2\Pi_{1/2}$ ladder have been detected at radio frequencies between 4 and 23 GHz (see Cesaroni & Walmsley 1991, for a summary of the observations and modeling). These lines probe levels with energies up to 511 K above ground, whose populations are determined by an interplay of strong far-infrared (FIR) radiation from warm dust and collisions in dense gas since the FIR rotational lines that (de)populate them, at frequencies > 1.8 THz, have high critical densities. Radiative transfer calculations show that many of them are not in local thermodynamic equilibrium (LTE), which gives rise to maser emission in some lines and enhanced absorption, caused by “overcooling”, in others, see Cesaroni & Walmsley (1991). As these authors show, just the fact that some lines do show maser emission and others do not places interesting constraints on kinetic temperature and density.

The modeling of the various cm OH hfs lines delivers a consistent picture of the OH in warm, dense gas. Nevertheless, for a full characterization, observations of the *rotational* OH transitions connecting hfs levels from different rotationally excited states are desirable. The frequencies of these transitions, within the $^2\Pi_{3/2}$ and $1/2$ ladders, and also between them, all lie in the supra-THz range. Using the Kuiper Airborne Observatory (KAO), Storey et al. (1981) made the first detection of the $^2\Pi_{3/2}, J = 5/2 - 3/2$ ground-state transitions near 2.51 THz ($119.3 \mu\text{m}$) in absorption toward Sgr B2 and in emission from the shocked gas in the Kleinmann-Low (KL) nebula in the Orion molecular cloud 1. Detections of other OH lines followed, including those of the other lines discussed in the present *Letter*, the $^2\Pi_{1/2}, J = 3/2 - 1/2$ transitions near 1.83 THz ($164 \mu\text{m}$), also in Orion (Viscuso et al. 1985). The Infrared Observatory (ISO) brought a significant improvement in sensitivity, although neither in angular nor in spectral resolution. Again, studies concentrated on the exceptionally bright and extended sources Sgr B2 and Orion-KL. Multi-transition data afforded by ISO’s long wavelength spectrometer allowed detailed excitation studies of both sources in several hydroxyl isotopologes ($^{16,17,18}\text{OH}$) (Goicoechea & Cernicharo 2002; Goicoechea et al. 2006; Polehampton et al. 2003).

Herschel and SOFIA have brought vast improvements over both the KAO and ISO in terms of sensitivity and angular and velocity resolution. Both are flying heterodyne spectrometers affording bandwidths of several hundred km s^{-1} even at THz frequencies and velocity resolutions better than 1 km s^{-1} , namely the Heterodyne Instrument for the Far Infrared (HIFI, de Graauw et al. 2010) and the German Receiver for Astronomy at Terahertz frequencies (GREAT¹, Heyminck et al. 2012). The increased sensitivity allows studies of more compact regions, namely the above mentioned dense molecular envelopes associated with UCHIIRs and OH masers. Recently, Wampfler et al. (2011) presented HIFI observations of the $^2\Pi_{1/2}, J = 3/2 - 1/2$

triplet of OH hfs transitions at 1837.8 GHz ($163.1 \mu\text{m}$) toward the high-mass star-forming region W3 IRS 5, for the first time resolving the hfs structure. A multi-rotational OH line study of the Orion Bar photon-dominated region with the PACS instrument onboard Herschel was presented by Goicoechea et al. (2011). Here we report in Sec. 2 our SOFIA observations of emission in this and the other Λ -doublet component at 1834.7 GHz ($163.4 \mu\text{m}$) toward the well-known UCHIIRs/OH maser sources W3(OH), G10.62–0.39 and NGC7538. The latter two have similar warm, dense molecular environments, and also show radio OH maser emission (Argon et al. 2000) and absorption (Walmsley et al. 1986). Toward the latter source we also observed absorption from the $^2\Pi_{3/2}, J = 5/2 - 3/2$ ground-state transitions near 2.51 THz ($119.3 \mu\text{m}$).

2. Observation and data reduction

The OH $^2\Pi_{1/2}, J = 3/2 - 1/2$ rotational lines were observed with the PI-instrument GREAT onboard SOFIA. The observations were carried out during flights no. SS02–OCF4/03 and BS02–01/06/07. The signal was detected at 1837.8 GHz ($163.1 \mu\text{m}$) using the L2 band of GREAT, while the pair of transitions from the other Λ -doublet at 1834.7 GHz ($163.4 \mu\text{m}$) lies in the image sideband. The beam is $15''.5$ at 1837.8 GHz. The AFFT backend was used with 1.5 GHz bandwidth and 212 kHz spectral resolution. The average system temperature is 4700–5300 K. Toward NGC 7538 IRS1 the $^2\Pi_{3/2}, J = 5/2 - 3/2^+$ rotational line at 2514 GHz was observed using the M-band receiver. See Wiesemeyer et al. (2012) for details of these observations. The pointing was established with the optical guide cameras (with an accuracy of $5''$).

The data were calibrated using standard procedures based on the KOSMA/GREAT calibrator (Guan et al. 2012), for the data analysis the GILDAS² software was used. The forward efficiency was set to 95% and the data were converted to a Rayleigh-Jeans equivalent $T_{\text{mb,RJ}}$ scale using a beam efficiency of 51% for the L2 and 58% for the M band, respectively.

The spectra were first summed up to define windows excluding the line signal for the baseline fitting. Then a third order polynomial baseline was fitted and subtracted from each scan individually. The $^2\Pi_{1/2}, J = 3/2 - 1/2$ spectra were averaged with noise weighting and are smoothed to $\sim 1.2 \text{ km s}^{-1}$. We reach on average ~ 0.3 – 0.4 K noise level per channel. The $^2\Pi_{3/2}, J = 5/2 - 3/2^+$ line was reduced in a similar fashion. Here, the spectrum is smoothed to 0.9 km s^{-1} velocity resolution and has a 0.4 K noise level.

3. Results

The Λ -doublet lines of the OH $^2\Pi_{1/2}, J = 3/2 - 1/2$ rotational transitions are detected, and as is characteristic of this transition, they are seen in emission (Fig. 1) toward all three high-mass star-forming sites. The $F = 2^+ - 1^-$ and $F = 1^+ - 0^-$ hfs components (at 1837.8168 and 1837.8370 GHz, respectively) are separated by 3.2 km s^{-1} and are therefore spectrally marginally resolved. The more separated and weaker $F = 1^+ - 1^-$ component (at 1837.7466 GHz) would be spectrally resolved, but lies within the noise level toward W3(OH) and NGC 7538 IRS1. Because GREAT is a double-sideband receiver, the other component of the Λ -doublet (a blended triplet at 1834.7355, 1834.7474, 1834.7504 GHz, for the $F = 1^- - 1^+, 2^- - 1^+, 1^- - 0^+$ transitions, respectively) could be recorded in the image band. For

¹ German Receiver for Astronomy at Terahertz frequencies. GREAT is a development by the MPI für Radioastronomie and the KOSMA/Universität zu Köln, in cooperation with the MPI für Sonnensystemforschung and the DLR Institut für Planetenforschung.

² See <http://www.iram.fr/IRAMFR/GILDAS/>

Table 1. Summary of the derived line parameters of the ${}^2\Pi_{1/2}, J = 3/2 - 1/2$ transition

Source	Position		$T_{mb,RJ}$ [K]	v_{lsr} km s $^{-1}$	Δv km s $^{-1}$	total τ	T_{ex} [K]
	RA[J2000]	Dec[J2000]					
W3(OH)	02:27:03.90	61:52:24.6	1.83 \pm 0.34	-45.70 \pm 0.31	7.54 \pm 0.87	0.1 – 2	40.2 – 5.1
G10.62–0.39	18:10:28.64	-19:55:49.5	1.34 \pm 0.29	-3.17 \pm 0.51	9.50 \pm 1.15	0.1 – 5	30.2 – 3.7
NGC7538 IRS1	23:13:45.36	61:28:10.5	1.04 \pm 0.34	-57.80 \pm 0.43	5.46 \pm 1.00	0.1 – 5	24.1 – 3.5

Notes. Line intensities are derived for the sum of the three hfs lines in each Λ -doublet of the ${}^2\Pi_{1/2}, J = 3/2 - 1/2$ transition. We give the range of total τ values that give fits within the noise level and the corresponding T_{ex} values. The total τ corresponds to the sum of optical depths of all hfs components in both doublet components.

G10.62–0.39 the $F = 1^+ - 1^-$ line partially overlaps with the emission from the image band.

For all sources, the observed line profiles of this transition exclude the presence of a broad outflow component within our noise level of ~ 0.4 K. The lines are turbulence-dominated and well-fitted with Gaussians within this noise level. The derived line-widths are consistent with those of other high-density tracers (Plume et al. 1997), suggesting an origin from a dense, turbulent medium.

Toward NGC 7538 IRS1, the blended 2514 GHz lines of the ${}^2\Pi_{3/2}, J = 5/2^- - 3/2^+$ rotational transition were also observed and are clearly seen in absorption. The triplet of lines from the other component of the Λ -doublet at 2510 GHz was not observed. The level of continuum emission was unstable and could not be determined reliably.

Given the OH molecules's substantial dipole moment (1.66 D), these high-frequency rotational transitions have high critical densities $\geq 10^8$ cm $^{-3}$. As a consequence, the LTE assumption is unlikely to apply even in the usual high-density environment of massive protostars, and FIR radiative pumping is expected to play a role in the excitation. Therefore ideally one should fit the individual hfs components to derive their intensity ratio, however, the presented spectra do not have sufficient signal-to-noise ratio for that. We used, hence, the HFS fitting method with CLASS and simultaneously fitted all six hfs components of the doublets with fixed optical depth, τ . Best fits, with a residual rms within the noise, are summarized in Table 1. The spectra's quality is moderate. For example, the broad feature underlying the 1837 GHz line toward W3(OH) is caused by an imperfect spectral baseline.

4. Analysis: Radiative transfer modeling

We used RATRAN (Hogerheijde & van der Tak 2000) to model OH emission from protostellar envelopes, where the effect of dust heating was included by adopting models from the literature (van der Tak et al. 2000; Mueller et al. 2002). Only for W3(OH) we present the ${}^2\Pi_{1/2}, J = 3/2 - 1/2$ line intensities calculated for a compact (few arcsecond size) source associated with OH maser emission with the large velocity gradient (LVG) model of Cesaroni & Walmsley (1991). In addition to the far-IR pumping, this takes into account line overlap effects and the hfs structure of the lines to give a detailed prediction for the cm radio lines of OH.

4.1. W3(OH): OH emission dominated by the UCHII region

Cesaroni & Walmsley (1991) created an LVG code³ to model the line properties (emission, absorption and population inversion) for the cm radio lines of OH toward W3(OH), where the 4 GHz

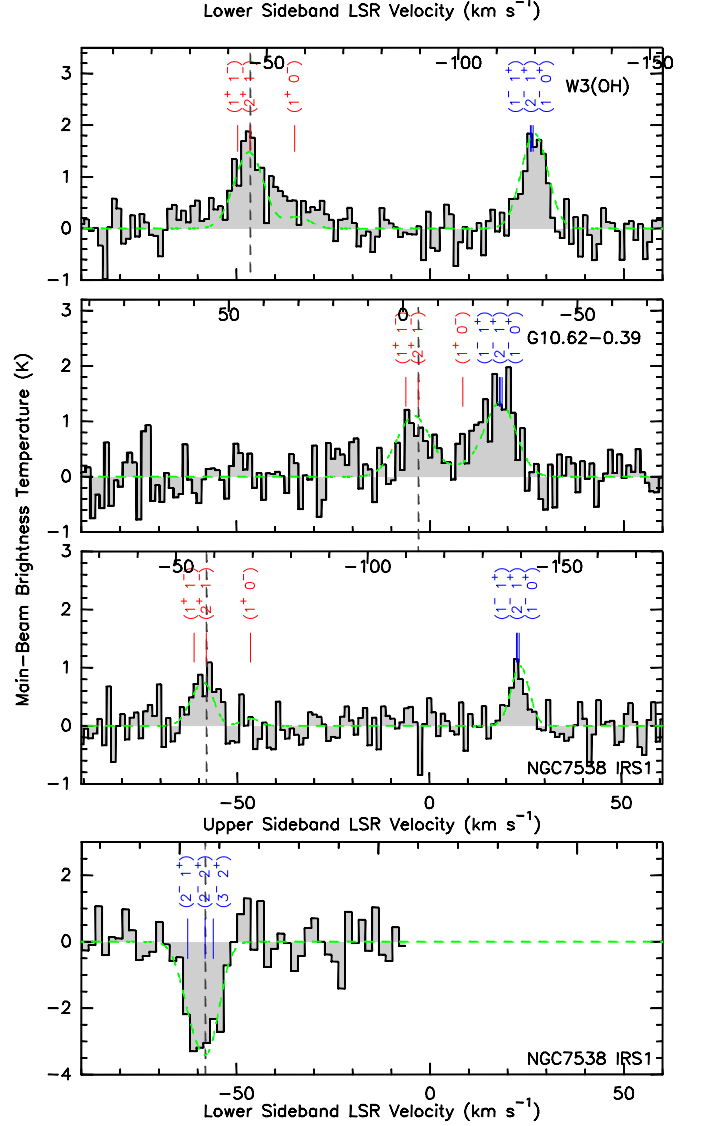


Fig. 1. Upper three panels: the ${}^2\Pi_{1/2}, J = 3/2 - 1/2$ rotational lines of the three UCHIRs in emission. The gray dashed line shows v_{lsr} . Red lines indicate the position of the hfs components of the - parity line of the doublet, while blue labels show the hfs of the + transition. (Labels are shifted for better visibility.) The dashed green line shows the $\tau = 0.1$ hfs fit to the spectra. The lower sideband rest velocity is shifted according to the v_{lsr} of the individual sources and is indicated on the upper axis of each plot, while the rest velocity scale is the same for all sources. The lowest panel shows the ${}^2\Pi_{3/2}, J = 3/2 - 5/2$ transition toward NGC 7538 IRS1.

³ This code uses the collisional cross-sections from Flower (1989).

hfs lines are seen in both emission and absorption. They show that this particular combination originates from a very narrow range of physical conditions. As a first step we reproduced their model and looked at the predictions for the far-IR lines.

The Cesaroni & Walmsley (1991) model describes a small (few arcsecond) compact source based on interferometric observations from the literature (Guilloteau et al. 1985, Wilson et al. 1990). They qualitatively reproduce the radio line observations using $T_{gas} = T_{dust} = 151$ K, including the presence of both internal dust and line overlap effects. The model uses an abundance, $\chi_{OH} = 2 \times 10^{-7}$ and a velocity gradient of $200 \text{ km s}^{-1} \text{ pc}^{-1}$ (see also App.A). Line overlap is taken into account and the velocity range available for non-local line overlap is fixed in this model to $\Delta V = 0.7 \text{ km s}^{-1}$. We reproduced their model and looked into the far-IR lines (Fig. A.1, upper panel). The observations agree well with the predictions of the model in a density range of $n_{H_2} = 2 - 3 \times 10^6 \text{ cm}^{-3}$ with a corresponding $T_{ex} \sim 50 - 60$ K. We note, however, that the model largely overpredicts the optical depth. Using this LVG code we also tested the importance of internal heating by dust, i.e. far-IR radiative pumping from the dust continuum photons. As shown in Fig. A.1 (lower panel) we find that models without a radiation field strongly underestimate the line intensity by an order of magnitude.

Because the known hot-core source, W3(H₂O), is only 6'' offset from W3(OH) (Wyrowski et al. 1999), we tested whether adding an envelope component could influence our model results. We used RATRAN (Hogerheijde & van der Tak 2000) and adopted an envelope model from van der Tak et al. (2000), with a power-law density profile $n(r) = n_0(r/r_0)^p$ ($n_0 = 5.3 \times 10^4 \text{ cm}^{-3}$, $p = -2$) and a temperature gradient with an exponent of -0.4 , adding up to a total luminosity of $2 \times 10^4 L_\odot$. We adopted an abundance of $\chi_{OH} = 0.8 \times 10^{-8}$, which is observed in a similar environment by Wampfler et al. (2011). These models predict very low line intensities ($T_L \sim 0.3$ K), therefore we conclude that for W3(OH) such an envelope model cannot significantly contribute to the observed line intensities. This result is consistent with the observed $v_{lsr} \sim -46 \text{ km s}^{-1}$ of the emission, which coincide with the UCHII region, W3(OH), rather than the neighboring hot-core, W3(H₂O).

4.2. NGC 7538 IRS1: OH emission dominated by an envelope component

For this source, the 2514 GHz ${}^2\Pi_{3/2}, J = 5/2 - 3/2$ transition was also observed. The line is seen in absorption and although the absorption feature seems to be saturated, the continuum level is uncertain. Hence, the only constraint we can deduce is that it appears in absorption. (The similar line-width of the hfs fits suggests that the optical depth may be similar to that of the ${}^2\Pi_{1/2}, J = 3/2 - 1/2$ transition.)

We used RATRAN to model an envelope with a power-law density and temperature profile with $n_0 = 5.3 \times 10^4 \text{ cm}^{-3}$, $p = -1.0$ and a total luminosity of $1.3 \times 10^5 L_\odot$ following van der Tak et al. (2000). Assuming a constant abundance of $\chi_{OH} = 0.8 \times 10^{-8}$ we reproduced the observed emission line intensities and the absorption feature as well (Fig. B.1). This indicates that an envelope model can explain rotational transitions of the emitting and absorbing OH gas.

4.3. G10.62–0.39: OH emission from an envelope and a compact source

Similarly as for the other sources, we produced models with RATRAN, where the physical model of the envelope is based on models of Plume et al. (1997) and Mueller et al. (2002), adopting a power-law density profile with an exponent $p = -2.5$, $n_0 = 1.2 \times 10^9 \text{ cm}^{-3}$ and a total luminosity of $9.2 \times 10^5 L_\odot$. These calculations produce a narrower emission feature than observed in our OH spectrum and underestimate the line intensity, giving $T_L \sim 0.6$ K. Either a higher OH abundance or the addition of a compact component corresponding to the UCHII region is needed.

5. Conclusions

We have detected the OH ${}^2\Pi_{1/2}, J = 3/2 - 1/2$ rotational lines in emission toward three classical UCHIIRs and the ${}^2\Pi_{3/2}, J = 3/2 - 5/2$ rotational line in absorption toward one of them, NGC 7538 IRS1. Our modeling shows that the far-IR radiation field plays an important role in the excitation conditions. Except for NGC 7538 IRS1, an envelope model with a low OH abundance ($\chi_{OH} = 0.8 \times 10^{-8}$) cannot explain the observed line intensities alone; an additional compact component with high density and high OH abundance is needed. We have shown for W3(OH) that the emission is dominated by the UCHIIR and not the nearby hot-core. Given the particular excitation properties of the radio lines of the OH molecule, a detailed modeling of their properties (emission, absorption, or population inversion) and observations of more rotational transitions of OH can provide more constraints on the physical conditions.

References

- Argon, A. L., Reid, M. J., & Menten, K. M. 2000, ApJS, 129, 159
 Barrett, A. H. & Rogers, A. E. E. 1966, Nature, 210, 188
 Cesaroni, R. & Walmsley, C. M. 1991, A&A, 241, 537
 Davies, R. D., Rowson, B., Booth, R. S., et al. 1967, Nature, 213, 1109
 de Graauw, T., Helmich, F. P., Phillips, T. G., et al. 2010, A&A, 518, L6+
 Dreher, J. W. & Welch, W. J. 1981, ApJ, 245, 857
 Flower, D. R. 1989, Phys. Rep., 174, 1
 Gardner, F. F., Robinson, B. J., Bolton, J. G., et al. 1964, Physical Review Letters, 13, 3
 Goicoechea, J. R. & Cernicharo, J. 2002, ApJ, 576, L77
 Goicoechea, J. R., Cernicharo, J., Lerate, M. R., et al. 2006, ApJ, 641, L49
 Goicoechea, J. R., Joblin, C., Contursi, A., et al. 2011, A&A, 530, L16
 Goss, W. M. 1968, ApJS, 15, 131
 Guan, X., Stutzki, J., Graf, U., et al. 2012, This issue
 Guilloteau, S., Baudry, A., & Walmsley, C. M. 1985, A&A, 153, 179
 Heyminck, S., Graf, U. U., Güsten, R., et al. 2012, This issue,
 Hogerheijde, M. R. & van der Tak, F. F. S. 2000, A&A, 362, 697
 Kawamura, J. H. & Masson, C. R. 1998, ApJ, 509, 270
 Mezger, P. G., Schraml, J., & Terzian, Y. 1967, ApJ, 150, 807
 Moran, J. M., Barrett, A. H., Rogers, A. E. E., et al. 1967, ApJ, 148, L69
 Mueller, K. E., Shirley, Y. L., Evans, II, N. J., et al. 2002, ApJS, 143, 469
 Plume, R., Jaffe, D. T., Evans, II, N. J., et al. 1997, ApJ, 476, 730
 Polehampton, E. T., Brown, J. M., Swinyard, B. M., et al. 2003, A&A, 406, L47
 Rogers, A. E., Moran, J. M., Crowther, P. P., et al. 1966, Physical Review Letters, 17, 450
 Storey, J. W. V., Watson, D. M., & Townes, C. H. 1981, ApJ, 244, L27
 van der Tak, F. F. S., van Dishoeck, E. F., Evans, II, N. J., et al. 2000, ApJ, 537, 283
 Viscuso, P. J., Stacey, G. J., Fuller, C. E., et al. 1985, ApJ, 296, 142
 Walmsley, C. M., Baudry, A., & Guilloteau, S., et al. 1986, A&A, 167, 151
 Wampfler, S. F., Bruderer, S., Kristensen, L. E., et al. 2011, A&A, 531, L16
 Weaver, H., Williams, D. R. W., Dieter, N. H., et al. 1965, Nature, 208, 29
 Weinreb, S., Barrett, A. H., Meeks, M. L., et al. 1963, Nature, 200, 829
 Weinreb, S., Meeks, M. L., & Carter, J. C. 1965, Nature, 208, 440
 Wiesemeyer, H., Güsten, R., Heyminck, S., et al. 2012, This issue,
 Wilson, T. L., Walmsley, C. M., & Baudry, A. 1990, A&A, 231, 159
 Wyrowski, F., Schilke, P., Walmsley, C. M., et al. 1999, ApJ, 514, L43

Acknowledgements. We are grateful to Riccardo Cesaroni for making his radiative transfer program available to us. We also thank the referee, J. Goicoechea, for a careful reading of the manuscript. This work was partially funded by the ERC Advanced Investigator Grant GLOSTAR (247078). Based on observations made with the NASA/DLR Stratospheric Observatory for Infrared Astronomy. SOFIA Science Mission Operations are conducted jointly by the Universities Space Research Association, Inc., under NASA contract NAS2-97001, and the Deutsches SOFIA Institut under DLR contract 50 OK 0901.

Appendix A: LVG model of W3(OH)

We reproduced the model of W3(OH) of Cesaroni & Walmsley (1991), which qualitatively models the radio lines of OH, and show here the predictions of this model for the 1834 and 1837 GHz lines. We adopted their parameters, assuming a source size of $2''$ (0.01 pc), a velocity gradient of 200 km s $^{-1}$ pc $^{-1}$ and an OH column density between 2×10^{14} cm $^{-2}$ to 2×10^{16} cm $^{-2}$. To compare these intensities with the observed values we used a beam size of $15''.5$ for SOFIA. In Fig. A.1 two models are shown, with and without an internal radiation field introduced by the present of warm dust. As shown, the latter model underestimates the observed line intensities.

This code is well-adapted for the OH molecule because it includes line-overlap effects, however, for a detailed modeling the radio OH lines need to be taken into account. To perform this modeling for all the sources is beyond the scope of this letter.

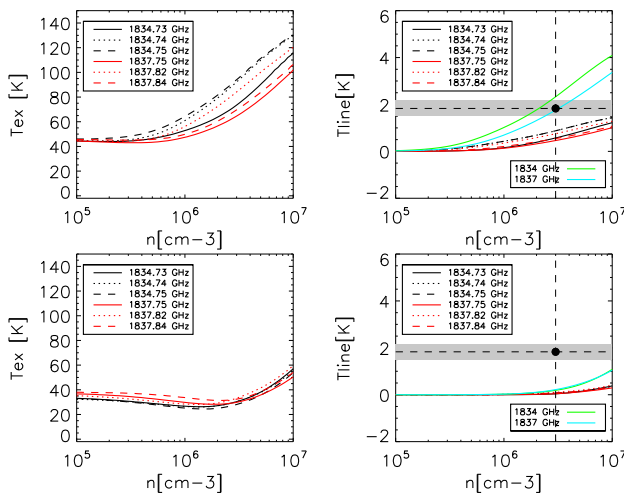


Fig. A.1. Results of the LVG models of Cesaroni & Walmsley (1991) showing only the predictions of excitation temperature and line intensity for the 1834 and 1837 GHz lines. The gray dashed area indicates the observed line intensity including the errors. Light green and blue lines correspond to the sum of the hfs lines in each component of the doublet. **Upper panels:** Models with internal radiation field. **Lower panels:** Models without internal radiation field.

Appendix B: RATRAN model of NGC7538 IRS 1

RATRAN is based on a Monte-Carlo approach to perform radiative transfer calculations (Hogerheijde & van der Tak 2000). It is therefore well-suited for detailed modeling of protostellar envelopes. A radiation field from dust heating was implemented in the models. Note that as shown in Fig. B.1, a line profile can be produced.

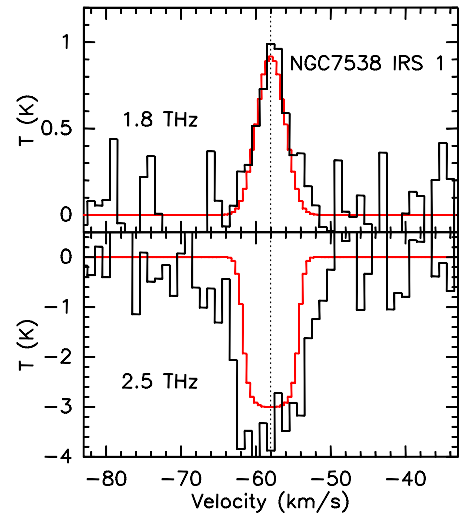


Fig. B.1. Our RATRAN model of the 1834 GHz and 2514 GHz OH line in emission and in absorption, respectively. Black line shows the observed spectra with baselines removed, the red line shows the model.